BBAA VI International Colloquium on:
Bluff Bodies Aerodynamics & Applications
Milano, Italy, July, 20-24 2008

THE OVERSHOOT OF AERODYNAMIC FORCES ON A RAILCAR-LIKE BODY UNDER STEP-FUNCTION-LIKE GUSTY WINDS

Takashi Takeuchi*, Junji Maeda*, and Hiromasa Kawashita*

* Kyushu University, 6-10-1 Hakozaki, Higashi-ku, Fukuoka 812-8581, Japan
e-mail: takeuchi@windmail.arch.kyushu-u.ac.jp,
maeda@wind.arch.kyushu-u.ac.jp,
kawashita@windmail.arch.kyushu-u.ac.jp

Keywords: Unsteady aerodynamic force, Short-time rising gust, Overshoot of wind force.

Abstract. *Although a wind force generated by a gust with a very short rise time differs from a quasi-steady aerodynamic force in consideration of small turbulent wind, it is less well known that a big wind force, which is not seen in a steady wind flow, acts on a structure as a transient phenomenon, except in the case of some research. This is because a specially-equipped wind tunnel is required in order to generate a gust with a short rise time. The development of such a big wind force is called the overshoot phenomenon of wind force. Systematized information on the overshoot of wind force is not yet available and its application to a structural design against such a gust does not start. This paper describes the effects of the short rise time of wind on the overshoot phenomenon of wind force acting on a railcar-like body using a specially-equipped wind tunnel which can generate a step-function-like gust. The wind tunnel is the Eiffel type of suction, the cross section length is 3m and the section size of the measurement part is 1.5m by 1.5m. The wind tunnel can generate a step-function-like gust adjusted as to a rise within 0.2 to 5 seconds from a calm state by control of the flat blade-rows used for generating a pulsation flow. We devised a special measure for the setting of a specimen on the measurement section of the wind tunnel, in order to eliminate the influence of the rapid pressure change of the inside and outside of the section accompanying the generated gust when measuring the lift of the specimen put on the floor. The results of our experiment showed that the most remarkable overshoot phenomenon appeared on the railcar-like body in the case of a gust with a shorter rise time and a lower wind speed generated the most notable overshoot phenomenon. Moreover, it was revealed that the overshoot coefficient which is defined by a ratio of the maximum to a steady-state value of the wind force is determined by the non-dimensional rise time which is composed of the rise time, the gust speed and the model size. Finally, an example of an observed natural gust which changed suddenly in a short time but not as a step-function-like gust was introduced. The non-dimensional rise time of a real train car under this wind was estimated using our experimental results, and it was shown that a stronger drag and lift of about 1.5 to 2.0 times the steady wind forces may have acted upon the vehicle.*

1 INTRODUCTION

Generally the wind load P of structural design is estimated by the following equation based on a quasi-static theory

$$P = \frac{1}{2}\rho C A U^2, \tag{1}$$

where, ρ: air density, C: wind-force coefficient, A: area, U: wind velocity.

Generally, the coefficient of wind force, C, is supplied by empirical data from wind tunnel tests under a stationary or small turbulent flow. The intensity of turbulence is, at most, about 20%, and the flow is classified as a quasi-steady flow. On the other hand, wind gusts such as those from tornadoes, downbursts, or big turbulent gusts have features different from quasi-steady winds such as those from typhoons or seasonal winds. These are especially characterized by the rise time of the wind. The wind force acting on a structure subjected to a gust with a very short rise time has some properties fundamentally differing from the quasi-static aerodynamic force.

Earlier reports [1-5] have shown that an overshoot phenomenon bringing a much bigger wind force than in a steady flow occurred in a structure subjected to a step-function-like gust. S. Taneda [1] measured the time-dependent lift acting on an elliptic cylinder rapidly started at an angle of attack using a water tank test. He reported that a remarkably big lift appeared just after starting, and then decreased immediately but increased up to a second peak before approaching a steady state gradually. T. Sarpkaya [2,3] showed that the laminar drag coefficient of a body grew up to about 25 percent higher during the growth of the first pair of vortices than in a steady flow, using an impulsive flow test over circular cylinders in a vertical water tunnel and adding some results of potential flow analyses around the circular cylinders. N. Shiraishi, et al., [4] evaluated unsteady aerodynamic characteristics using aerodynamic indicial functions. M. Matsumoto, et al., [5] measured a transient drag force on a two-dimensional cylindrical model under a suddenly-changing wind speed using a wind tunnel test with a working section of 200mm by 200mm square and reported an overshoot phenomenon in which the drag force increased by about 20 percent compared to the force in a steady flow. A force on a body in a wind flow with an acceleration was evaluated by a semi-empirical equation which added an inertia term proportional to its acceleration to Eq. (1) [6-11]. G. H. Keulegan and L. H. Carpenter [6] investigated the inertia and drag coefficients of cylinders and plates in a simple sinusoidal flow. Davenport [7] found that the inertia coefficient decreased with an increase in a reduced frequency. T. Sarpkaya [8], T. Sarpkaya and C. J. Garrison [9] investigated the inertia coefficient of a cylinder immersed in a two-dimensional uniform flow with constant acceleration. Y. K. Wen [10] reported that sudden change in wind velocity and direction due to a tornado induced a large inertia force in the tangential and radial directions near the ground. E. Savory [11] analyzed the damage of a lattice tower caused by tornados and downbursts using a model taking an inertia force into account. Both the inertia force induced by a tornado and the overshoot phenomenon of wind force induced by a suddenly-rising gust are transitional unsteady forces and generated by suddenly changed wind velocity.

As mentioned, several studies indicated that a big hydrodynamic force acted transiently on a body due to the suddenly-changing speed of a flow, but many of the reports used a water tank test. There are limited reports of an experiment using a wind tunnel that generates a gust rising in a short time. The development of such a big wind force is called the overshoot phenomenon of wind force. Since a specially-equipped wind tunnel is required in order to generate a gust with a short rise time, information on the rise time, wind speed and the size of the

body which must be related to the overshoot of the wind force has not yet been systematized, and its application to a gust resistant measure has not yet been attempted.

In this paper, we report the effects of the rise time of a step-function-like gust on the overshoot phenomenon of wind forces acting on the two-dimensional body of a box-section like a railcar using a specially-equipped wind tunnel to generate a short-rising gust. This wind tunnel is the Eiffel type of suction. The wind tunnel can generate a step-function-like gust adjusted so as to rise from a calm state within 0.2 to 1.4 seconds by controlling the rotation of flat blade-rows installed at a suction opening for generating a pulsation flow. We also devised a special measure for the setting of a specimen on the measurement section of the wind tunnel, in order to eliminate the influence of the rapid pressure change of the inside and outside of the section accompanying the generated gust in measuring the lift of the specimen put on the floor. Additionally, we tried an unsteady flow simulation of the experimental situation using k-ε model. Finally, an example of an observed natural gust which changed suddenly in a short time but not as a step-function-like gust was introduced and the effects of the overshoot phenomenon on a wind force acting on a real railcar were estimated.

2 GENERAL SPECIFICATIONS OF THE WIND TUNNEL TEST

2.1 Outline of experimental facility

We used a wind tunnel of the Eiffel type at Kyushu University. The site plan of our testing system is illustrated in Fig.(1). The section area of the working space was 1.5m by 1.5m and the available length was 3m. A step-function-like gust was generated by the following procedures using flat blade-rows for generating a pulsation flow. First, we shut the front blade rows shown in Fig.(1) to keep the working space calm during the fans' driving. Concurrently, we opened the top and bottom blade rows in order to avoid a negative pressure in the suction part. Secondly, we quickly opened all the front blade rows 90 degrees and simultaneously closed the top and bottom blade rows. Following this, an immediate flow came in to the working section and a step-function-like gust was generated. The rise time of the wind flow could be adjusted from the shortest 0.2 to 5 seconds by adjusting the speed of rotation of the blade rows. The tests were performed according to these procedures and the wind forces acting on the specimen were measured with the wind speed in the working space at the same time. An example of the time evolution of the wind velocity generated by control of the blade rows is shown in Fig.(2). The rise time of gust, t_r, is defined as the time an approaching wind required to reach a target wind, and the target wind velocity, U_t, is referred as the reached wind. The selected variables in our tests are listed in Table 1. The wind forces acting on the specimen were measured using an aerodynamic balance, and the wind speed in the working space was confirmed by a hot-wire anemometer and an ultrasonic anemometer, respectively. The measured data was recorded for 15 seconds, scanning at a frequency of 2000 Hz.

Table 1: Experimental variables

Target wind velocity U_t (m/s)	3.5, 5.0, 7.0, 10.0, 15.0
Rise time t_r (sec)	0.2, 0.3, 0.4, 0.6, 0.8, 1.0, 1.4

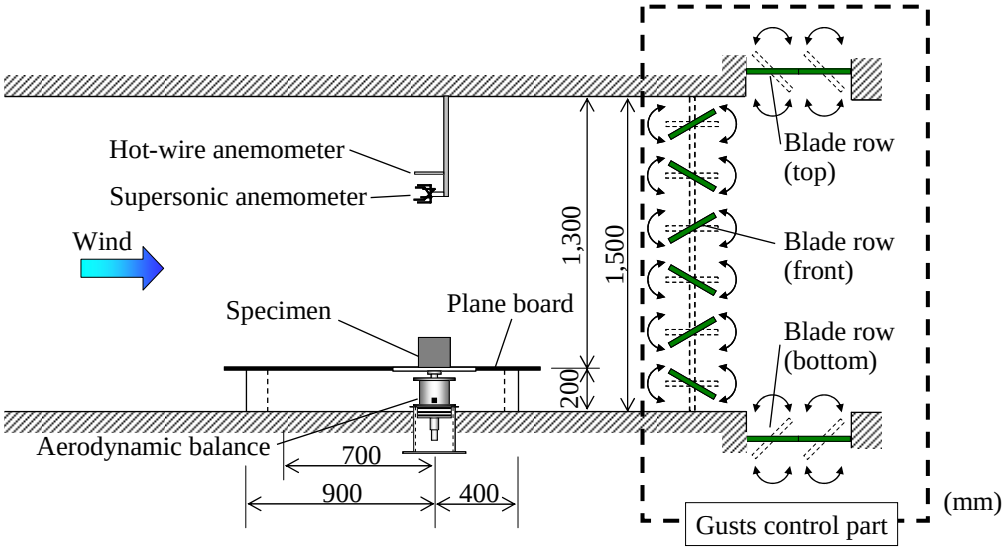

Figure 1: Site plan of the wind tunnel.

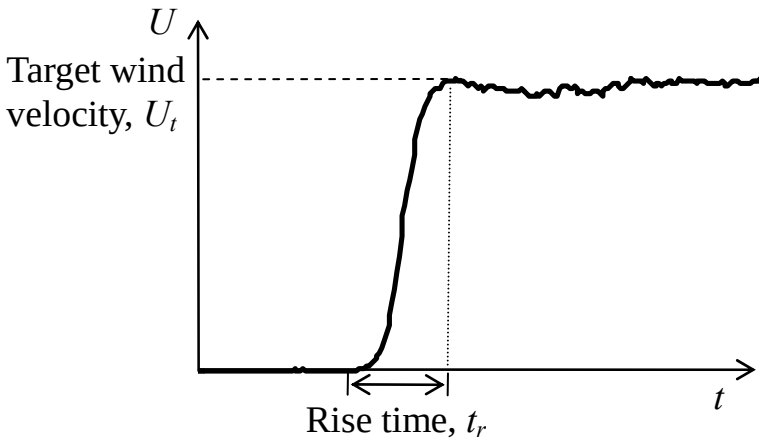

Figure 2: Example of the time evolution of the wind velocity measured under the step-function-like gust.

2.2 Devices of Installation of Test Body

Our test body was a railcar-like body with a 90mm high box-section of 74mm width and 500mm depth with one-sided round edges. This test body was fixed to the aerodynamic balance, and the drag and lift forces acting on the body were measured. We put the test body on a plane board 200mm off the floor of the wind tunnel so that the effects of the wind profile near the floor were eliminated, and covered the balance using a boat-shaped box. However, we found the following difficulty with the mounting of the test body. Fig.(3b) shows the time evolutions of Fx-, Fy- and Fz-components of the balance when a step-function-gust was generated without the test body, as shown in Fig.(3a). Here Fx, Fy and Fz are defined as shown in Fig.(3a). The components of Fx and Fy are almost 0 but the component of Fz shows an overshoot phenomenon even though the body is not yet installed. This is because a rapid change of the inside pressure of the wind tunnel caused by a rapid change of wind strongly affects the z-component of the balance which is outside the wind tunnel. Consequently, we must assume that the z-component of the balance indicates a lift component affected by the rapid change of the inside pressure of the wind tunnel in this case. It is difficult to measure only the lift on the test body. In order to eliminate this difficulty, we fixed a perpendicular plane board as the ground plane on the board fixed 200mm above the wind tunnel floor and tried to connect the

test body perpendicularly with the balance very close to the perpendicular board, as shown in Fig.(4a). Fig.(4b) shows the time evolutions of the output signals of the balance when a step-function-gust is generated without the test body in the condition as shown in Fig.(4a). The corresponding time evolutions in Fig.(4b) to those in Fig.(3b) indicate that the added perpendicular plane board has little influence on the output signals of the balance. We thought that if we measured by connecting the test body perpendicularly with the balance very close to the board, and took the corresponding Fx and Fy as the drag and lift of the body respectively, the influence of the rapid change of pressure would be avoidable. The test body was separated by about 1mm from the perpendicular plane board equivalent to the ground plane, as shown in Fig.(5a), so that the balance would not measure the wind forces acting on the board. Additionally, a dummy affixed to the board to realize a two-dimensional flow around the test body was placed at a distance of 3mm from the body, as shown in Fig.(5b). The blockage rate of the body, including several added devices, was 6.53% for the cross section of the measurement area. We report the results of our experiment under the situation shown in Fig.(5) in the next section, in which the drag and lift of the test body are shown as the Fx component and Fy component of the aerodynamic balance.

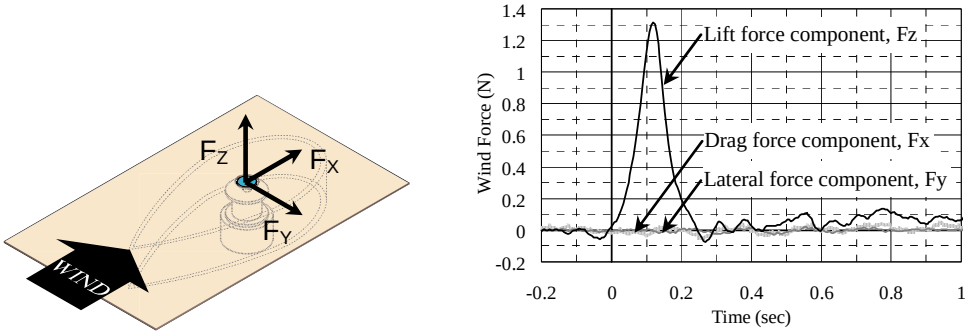

a) Directions of the measured forces. b) Time histories of the forces measured by the balance.

Figure 3: Time histories of the forces measured by the balance without the test body.

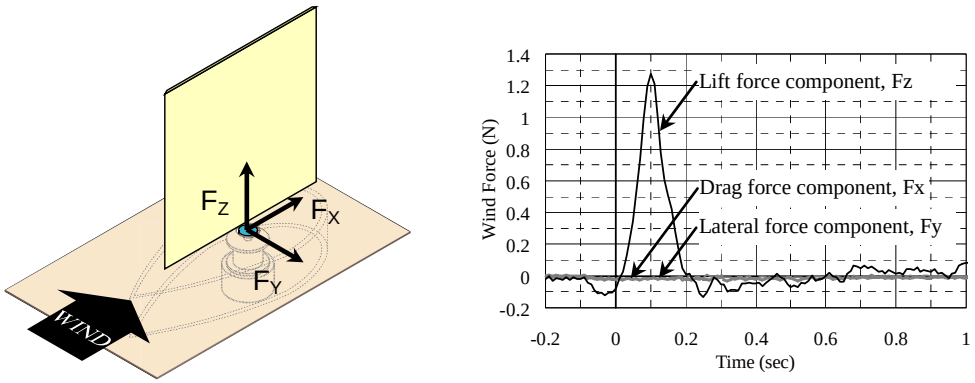

a) Directions of the measured forces. b) Time histories of the forces measured by the balance.

Figure 4: Time histories of the forces measured by the balance without the test body under a fixed perpendicular board.

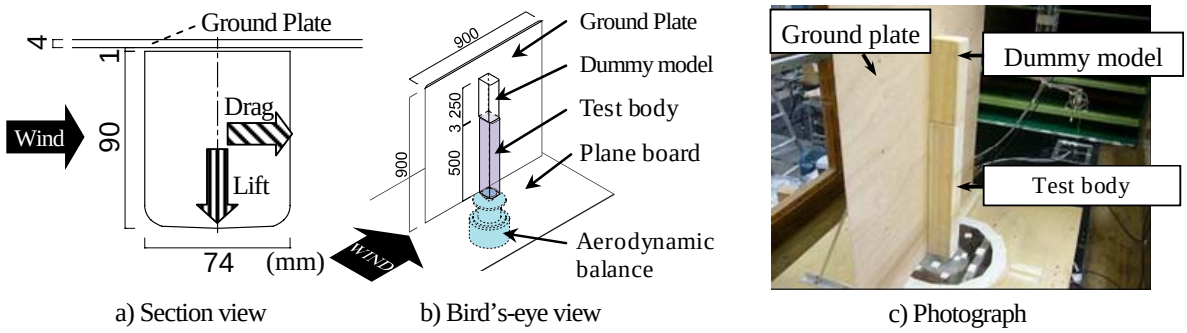

a) Section view b) Bird's-eye view c) Photograph

Figure 5: Specimen.

3 EXPERIMENTAL RESULTS AND DISCUSSIONS

3.1 Overshoot of wind forces

Fig.(3) shows the time evolutions of the wind velocity, and the drag and lift forces, when the target wind velocity reached 3.5m/s in a rising time of 0.2 sec, and 1.4 sec. The time axis was arranged so that the wind velocity began to rise at 0 sec, and the 3-second time range from the measured data is illustrated in Fig.(3). In the case of the rise time of 1.4 seconds, we did not see the overshoot phenomenon. On the other hand, in the case of the rise time of 0.2 seconds, we saw an overshoot phenomenon of the aerodynamic forces, which reached much larger values than the steady values of the drag and lift. However, the values decreased at once, and settled down in the stationary state. The peaks of the drag and lift forces occurred at about the same time as the wind velocity reached the target value. These results correspond to the first peak of the time history of the lift in Taneda's report [1].

3.2 The effect of the rise time and the target wind velocity on the overshoot phenomenon.

In order to verify the validity of the experiment, we calculated the coefficient of the wind force in a steady flow. The steady value was defined as a mean of 5 seconds after the overshoot settled down. Figs.(7a) and (7b) show the steady values of the drag and lift and their wind coefficient according to the target wind velocity. The left longitudinal axis of these graphs expresses the wind force and the right longitudinal axis expresses the coefficient. The steady drag coefficient (a continuous line in Fig.(7a)) is about 0.92 regardless of the target velocity. The steady lift coefficient (a continuous line in Fig.(7b)) decreased with an increase in the target wind velocity, and the values ranged from 0.2 to 0.4. These coefficients approximately correspond to the wind force coefficients of the experiment in Ref. [12].

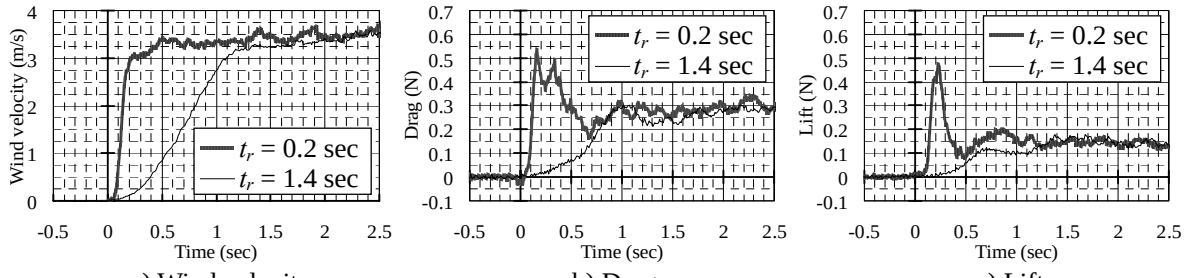

a) Wind velocity b) Drag c) Lift

Figure 6: The time history data (U_t = 3.5 m/s).

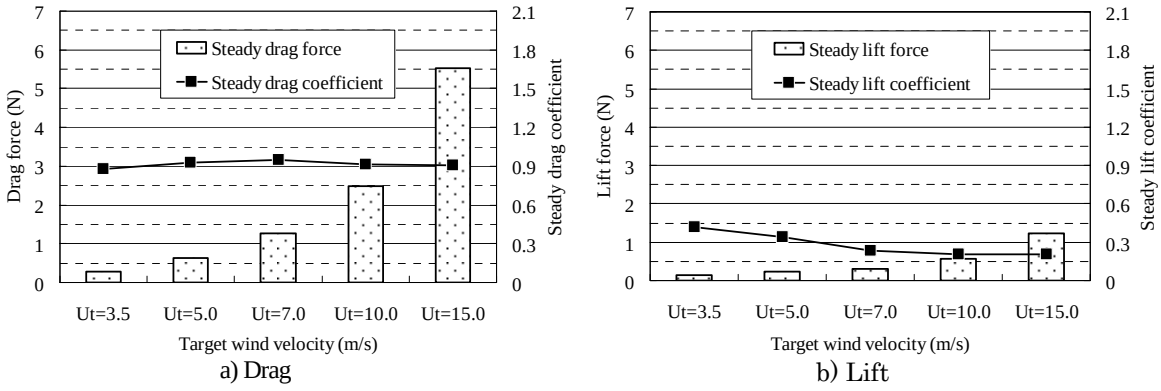

Figure 7: The steady values and the wind-force coefficients with the target wind velocity.

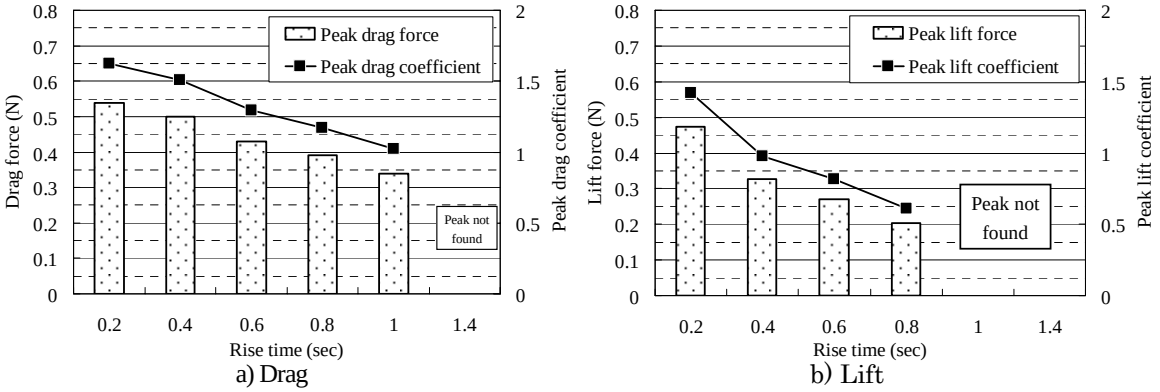

Figure 8: The peak values and the wind-force coefficients with the rise time (U_t = 3.5 m/s).

Fig.(8) shows the relationship between the peak value of the wind force and the rise time in the case of a target wind velocity of 3.5 m/s and clarifies the impact of the rise time on the overshoot phenomenon. This figure also includes the wind force coefficient to the peak value. We describe the wind force coefficient to the peak value as the peak wind force coefficient. The peak wind force coefficient is defined by the reference area of the model and the steady velocity pressure, as shown in the following equation

$$Peak\ wind\ \ force\ coefficient = \frac{Peak\ wind\ \ force}{0.5\rho\bar{U}^2 A}, \tag{2}$$

where, A is the reference area of the model, $\bar{U}$ is the steady wind velocity.

In the case of the rise time of over 1.4 seconds in Fig.(8a) and in the case of the rise time of over 1.0 seconds in Fig.(8b), the peak wind force coefficients are not shown, since a peak value higher than a steady value could not be confirmed. The peak value and the peak wind force coefficient decrease with an increase in the rise time. The change of the peak lift coefficient to the rise time is larger than the change of the peak drag coefficient to the rise time. In the case of a target wind velocity of other than 3.5 m/s, the peak wind forces and the peak wind force coefficients show the same tendency of decreasing with an increase in the rise time.

Fig.(9) shows the peak value of the wind force and the peak wind force coefficient in the case of the rise time of 0.2 seconds. Beyond doubt, the peak values increase with an increase in the target wind velocity. On the other hand, the peak wind force coefficients decrease with an increase in the target wind velocity. Fig.(10) shows the effect of the target wind velocity on the overshoot phenomenon with the overshoot coefficient defined by the ratio of the peak value to the steady value. The overshoot coefficient increases with a decrease in the target

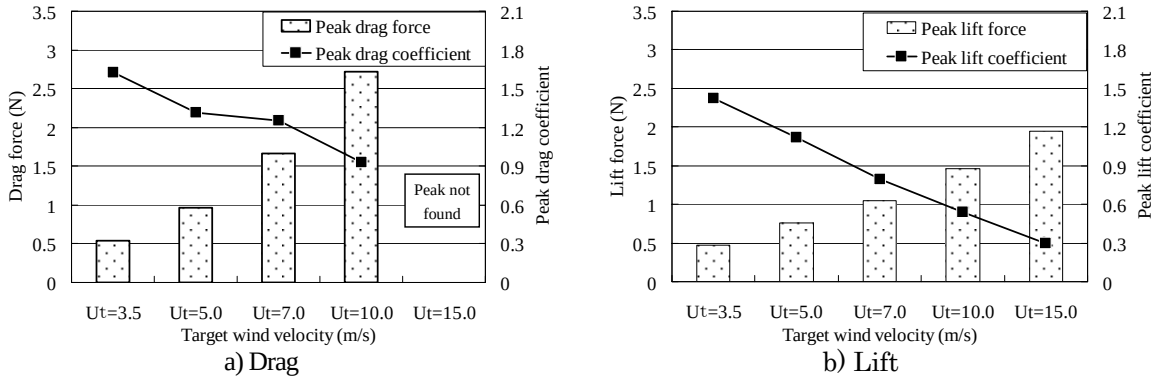

Figure 9: The peak values and the wind-force coefficients with the target wind velocity (t_r = 0.2 sec).

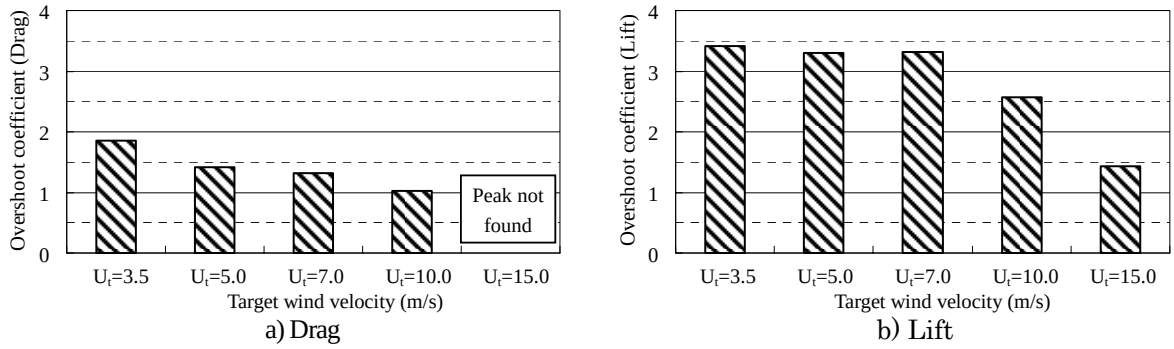

Figure 10: The overshoot coefficients with the target wind velocity (t_r = 0.2 sec).

wind velocity in the case of the rise time of 0.2 seconds. In the case of the target wind velocity of 3.5m/s, the peak drag was about 1.8 times larger than the steady drag, and the peak lift was about 3.4 times larger than the steady lift. The overshoot phenomenon occurs most obviously on the lift.

3.3 Relationship between the overshoot coefficient and the non-dimensional rise time

We analyzed the overshoot phenomenon with the peak wind force coefficient and the overshoot coefficient in the preceding section. Since the steady wind force coefficient was almost constant in value regardless of the target wind velocity, the peak wind force coefficient and the overshoot coefficient showed the same tendency as that for the rise time and the target wind velocity. In what follows, we investigated the overshoot phenomenon with the overshoot coefficient. It was confirmed that the overshoot phenomenon clearly appeared in both the drag and the lift when the rise time was very short and that the overshoot coefficient increased with a decrease in the target wind velocity. To compare the overshoot in the various rise times and target wind velocities, the non-dimensional time, t', was defined by Eq. (3) in reference to Ref. [1]

$$t' = U_t \cdot t / d, \tag{3}$$

where, U_t is the target wind velocity, t is time and d is a reference length (here, the width of the model).

Fig.(11) shows the non-dimensional time evolutions of the wind velocity, and the drag and lift forces, when the target wind velocity reached 3.5m/s and 5.0m/s in the rising time of 0.2 seconds. Fig.(11a) shows that the non-dimensional time period taken for the wind velocity to

rise in the case of the target wind velocity of 3.5m/s was shorter than in the case of the target wind velocity of 5.0m/s. Taneda [1] reported that at the initial stage after an elliptic cylinder started, the convection and the viscous terms in Navier-Stokes equation could be cut because Ut/d and vt/d^2 are considerably small, and then a potential flow was formed and the lift on the elliptic cylinder became big. For this reason, we think that the overshoot phenomenon is affected by the non-dimensional time taken for the wind velocity to rise and defined the non-dimensional rise time, t_r', by Eq. (4)

$$t_r' = U_t \cdot t_r / d, \tag{4}$$

where, t_r is the rise time of the wind.

Fig.(12) shows the relation between the non-dimensional rise time and the overshoot coefficient and clarifies the tendency of the overshoot coefficient to decrease with an increase in the non-dimensional rise time. Fig.(13) converts Fig.(12) into an expression using logarithmic axes. The data are spread out because of a lack of experiments, but indicate that the relation between the overshoot coefficient and the non-dimensional time could be approximated by a power index. The continuous line in the figure is a regression line, which is obtained by the method of least squares. The coefficient of correlation is -0.717 on the drag and is -0.957 on the lift. Both the coefficients of correlation on the drag and the lift are high, and, in particular, the coefficient of correlation on the lift is very high. The relation between the overshoot coefficient and the non-dimensional rise time can be applied in evaluating the wind load on a structure subjected to a step-functional-gust.

4 TRIAL VERIFICATION BY CFD ANALYSIS

We tried a CFD analysis of the above-mentioned experimental results using the PISO (Pressure-Implicit with Splitting of Operators [13-15]) method and the standard k-ε model of turbulence. We made a model of an analytical region around the test body, as shown in Fig (14), where a two-dimensional flow was assumed. The short-time-rising wind velocity measured in the wind tunnel test was modeled on an approaching flow in the CFD simulation, as shown in Fig.(15), which is almost 0 in the first interval, then is expressed by a cubic function until reaching a constant target wind at the rise time.

Fig.(16) shows the comparisons between the CFD calculation and experimental results in the case of a target wind velocity of 3.5m/s and a rising time of 0.2 seconds. Both drag and lift estimated by the simulation were bigger than the experimental results, but the overshoot phenomenon can be confirmed in the simulation as well as in the experimental results.

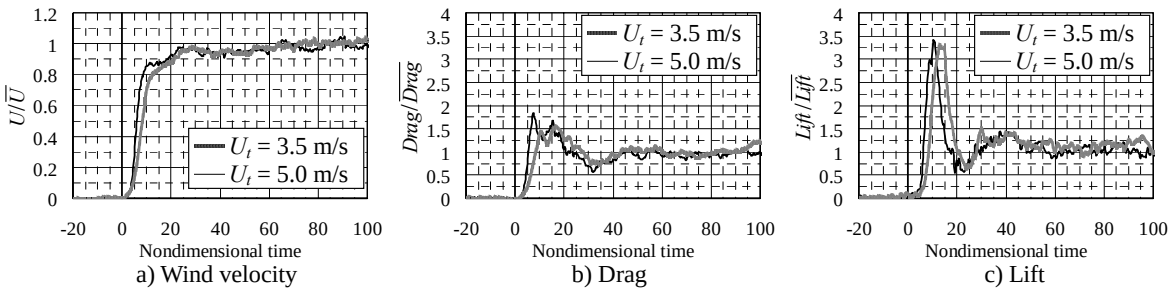

Figure 11: The non-dimensional time history data (t_r = 0.2 sec).

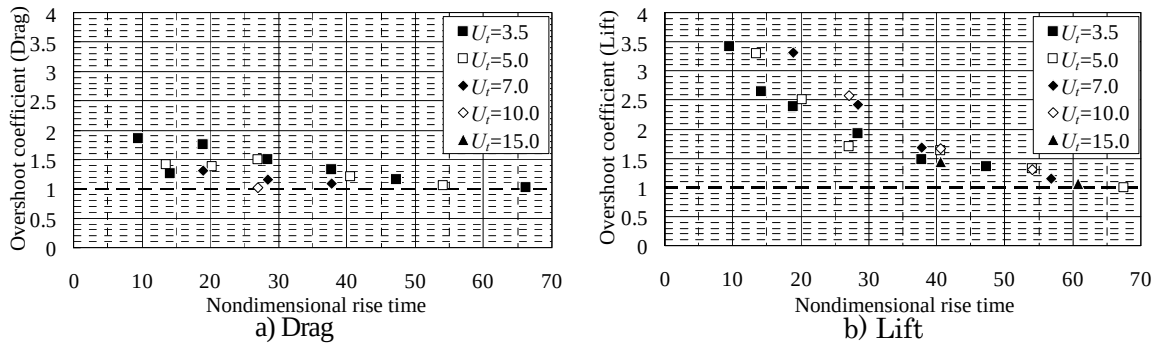

Figure 12: The relationships between the overshoot coefficient and the non-dimensional rise time.

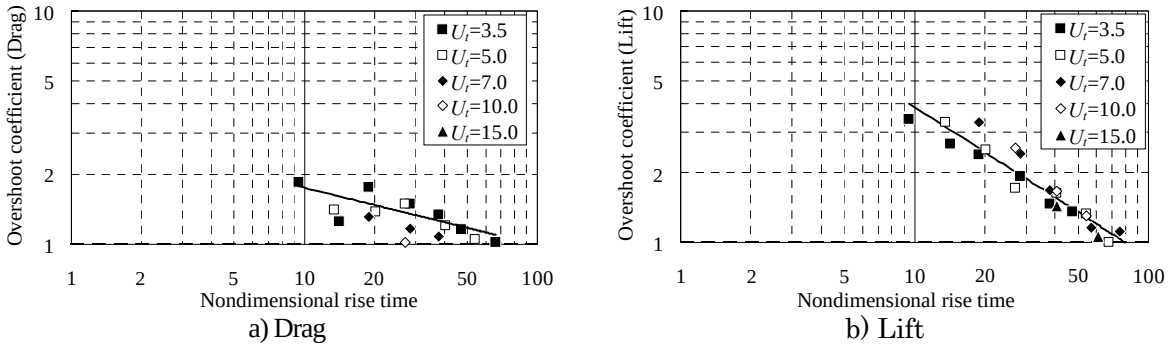

Figure 13: The relationships between the overshoot coefficient and the non-dimensional rise time (logarithmic axes).

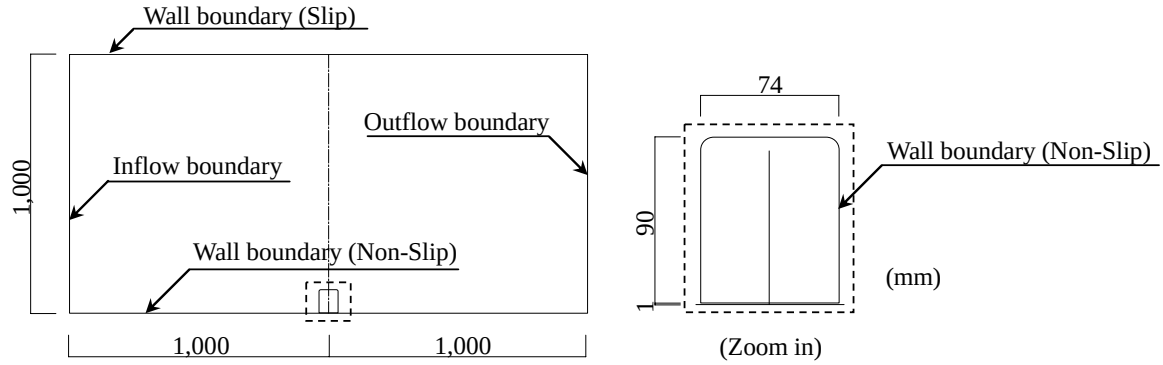

Figure 14: The analytic region.

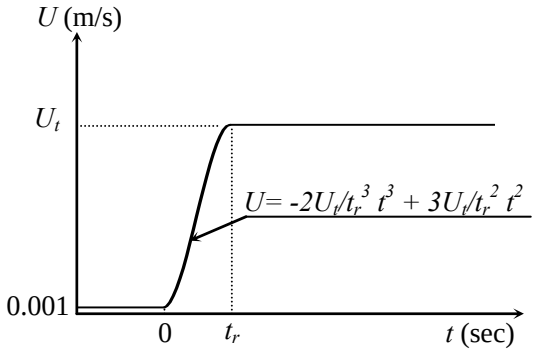

Figure 15: The inflow wind velocity.

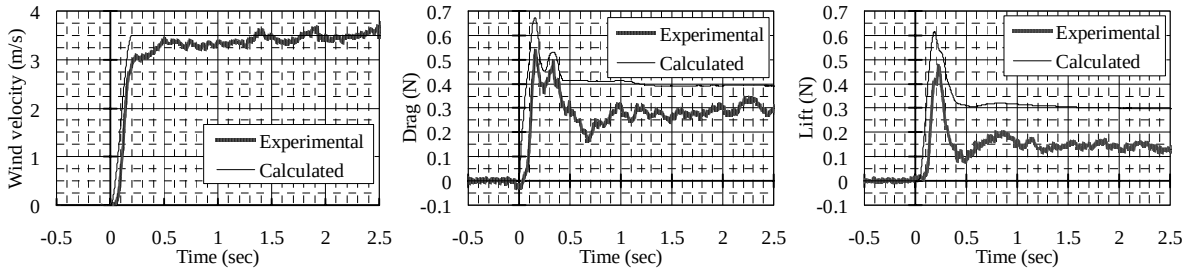

a) Wind velocity b) Drag c) Lift

Figure 16: Comparisons between the calculated result and the experimental result (U_t = 3.5 m/s, t_r = 0.2 sec).

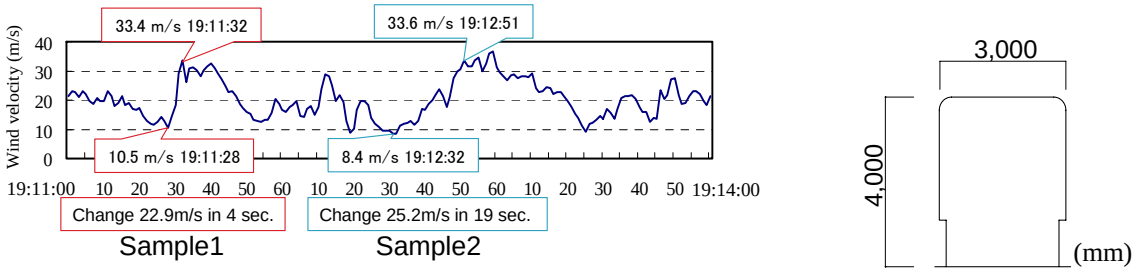

a) The time history of wind velocity measured at NeWMeK (19:11~19:14). b) Section of derailed railcar

Figure 17: The time history of wind velocity measured at NeWMeK and the section of the derailed railcar.

5 APPLICATION TO AN OBSERVED WIND RECORD

A derailment accident of a railcar which was moving slowly near a railway station in Fukuoka City, Japan, occurred due to a gust in March 1998. At that time the gusts around this accident site happened to be recorded at a site of NeWMeK (Network for Wind Measurement in Kyushu [16-17]), which was located 500m windward from the site. The time evolutions of 1-second-averaged wind speed recorded at the NeWMeK site when the accident occurred at 7:11 p.m. are shown in Fig.(17a). We can see a rapid change over 4 seconds of about 20m/s of wind speed at 7:11:28 p.m. before a slow one over 20 seconds at 7:12:32 p.m. Here these rapid and slow changes of wind are called “sample1” and “sample2”, respectively. Taking into account the size of the derailed railcar of 3m in depth in Fig.(17b), we can estimate the non-dimensional rise times of sample1 and sample2 using Eq. (4) as 31 and 162 respectively. Referring the non-dimensional time of sample1 to Fig.(12), it is estimated that the overshoot coefficient of drag is about 1.5 and the one of lift is about 2.0. In the case of sample2, both overshoot coefficients of drag and lift are 1.0. It is thought that the overshoot phenomenon didn't occur in the case of sample2 but the railcar in the case of sample1 might have been subjected to about 1.5-2.0 times wind force in comparison with the steady force.

6 CONCLUSIONS

Several features of transient wind forces acting on a railcar-like body subjected to a step-function-like gust were investigated using a specially-equipped wind tunnel, which can generate the gust of a rise time of 0.2 to 5 seconds from a flat calm by controlling the rotation speed of the blade rows. A special measure was devised for setting a test body on the measurement section in the wind tunnel in order to eliminate the influence of a rapid change of the inside pressure on a lift force acting on the body. This revealed the features of the transient wind forces acting on the railcar-like body subjected to a short-time-rising gust as follows:

- We confirmed an overshoot phenomenon bringing a much bigger wind force than in a steady flow. The overshoot phenomenon was more remarkable in the case of a gust with a shorter rise time.
- The overshoot phenomenon correlates strongly with the rise time of wind and the target wind speed, and develops with a decrease in the rise time or the wind speed.
- The overshoot coefficient defined by a ratio of a maximum to a steady-state value of wind force is determined by a non-dimensional rise time which is composed of a rise time, a gust speed and the body size.
- We tried an unsteady flow simulation of the experimental situation using a CFD k-ε model and confirmed that the CFD simulation results show some overshoot phenomena almost equivalent to our experimental results.
- An example of an observed natural gust was introduced which changed suddenly in a short time but not as a step-function-like gust in the wind tunnel test. The non-dimensional rise time of a real train car under such a gust was estimated using our experimental results and it was found that a stronger drag and lift of about 1.5 to 2.0 times the steady wind forces may have been generated.

REFERENCES

[1] S. Taneda. The Development of the Lift of an Impulsively Started Elliptic Cylinder at Incidence. *Journal of the Physical Society of Japan*, **33**, 1706-1711, 1972

[2] T. Sarpkaya. Separated Flow about Lifting Bodies and Impulsive Flow about Cylinders. *AIAA Journal*, **4**, 414-420, 1966.

[3] T. Sarpkaya. An Analytical Study of Separated Flow about Circular Cylinders. *Trans. of ASME, J. of Basic Eng.*, **90**, 511-520, 1968.

[4] N. Shiraishi, M. Matsumoto and H. Shirato. A Fundamental Study about Unsteady Aerodynamic Characteristics of Structures due to Fluctuating Wind. Proceedings of JSCE, No.328, 19-30, 1982.

[5] M. Matsumoto, M. Shimamura, T. Maeda, H. Shirato, T. Yagi, K. Hori, Y. Kawashima and M. Hashimoto. Drag forces on 2-D cylinders due to sudden increase of wind velocity. 12th International Conference on Wind Engineering, Preprints-Vol.2, 1727-1734, 2007.

[6] G. H. Keulegan and L. H. Carpenter. Forces on Cylinders and Plates in an Oscillating Fluid. *Journal of Research of the National Bureau of Standards*, **60**, 423-440, 1958.

[7] A. G. Davenport. The Application of Statistical Concepts to the Wind Loading of Structures. Proceedings of the Institution of Civil Engineers, Vol. 19, 449-472, 1961.

[8] T. Sarpkaya. Lift, Drag, and Added-Mass Coefficients for a Circular Cylinder Immersed in a Time-Dependent Flow. *Journal of Applied Mechanics*, **30**, 13-15, 1963.

[9] T. Sarpkaya and C. J. Garrison. Vortex Formation and Resistance in Unsteady Flow. *Journal of Applied Mechanics*, **30**, 16-24, 1963.

[10] Y. K. Wen. Dynamic Tornadic Wind Loads on Tall Buildings. *Journal of the Structural Division*, **101**, 169-185, 1975.

[11] E. Savory, G. A. R. Parke, M. Zeinoddini, N. Toy, P. Disney. Modelling of Tornado and Microburst-induced Wind Loading and Failure of a Lattice Transmission Tower. *Engineering Structures*, **23**, 365-375, 2001.

[12] C.J. Baker, J. Jones, F. Lopez-Calleja and J. Munday. Measurements of the cross wind forces on trains. *Journal of Wind Engineering and Industrial Aerodynamics*, **92**, 547–563, 2004.

[13] R. I. Issa. Solution of the Implicitly Discretised Fluid Flow Equations by Operator-Splitting. *Journal of Computational Physics*, **62**, 40-65 ,1985

[14] R. I. Issa, A. D. Gosman and A. P. Watkins. The Computation of Compressible and Incompressible Recirculating Flows by a Non-iterative Implicit Scheme. *Journal of Computational Physics*, **62**, 66-82 ,1986

[15] R. I. Issa, B. Ahmadi-Befrui, K. R. Beshay and A. D. Gosman. Solution of the Implicitly Discretised Reacting Flow Equations by Operator-Splitting. *Journal of Computational Physics*, **93**, 388-410 ,1991

[16] T. Fujii, J. Maeda, N. Ishida and T. Hayashi. An analysis of a pressure pattern in severe Typhoon Bart hitting the Japanese Islands in 1999 and a comparison of the gradient wind with the observed surface wind. *Journal of Wind Engineering and Industrial Aerodynamics*, **90**, 1555-1568, 2002.

[17] J. Maeda, N. Ishida. Wind distribution analyses using a measurement array of high density. Proceedings of the 14th National Symposium on Wind Engineering, Tokyo, Japan, December 4-6, pp. 1–6, 1996.